



12-1987

Kinetics of the Metal-Exchange Reaction between N-(2-Pyridylmethyl)Iminodiacetonickel(N) and Copper(II)

Kassahun W. Beyene

Follow this and additional works at: https://scholarworks.wmich.edu/masters_theses

 Part of the Analytical Chemistry Commons

Recommended Citation

Beyene, Kassahun W., "Kinetics of the Metal-Exchange Reaction between N-(2-Pyridylmethyl)Iminodiacetonickel(N) and Copper(II)" (1987). *Master's Theses*. 1233.
https://scholarworks.wmich.edu/masters_theses/1233

This Masters Thesis-Open Access is brought to you for free and open access by the Graduate College at ScholarWorks at WMU. It has been accepted for inclusion in Master's Theses by an authorized administrator of ScholarWorks at WMU. For more information, please contact wmu-scholarworks@wmich.edu.



**KINETICS OF THE METAL-EXCHANGE REACTION BETWEEN
N-(2-PYRIDYLMETHYL)IMINODIACETATONICKEL(II)
AND COPPER(II)**

by

Kassahun W. Beyene

**A Thesis
Submitted to the
Faculty of The Graduate College
in partial fulfillment of the
requirements for the
Degree of Master of Arts
Department of Chemistry**

**Western Michigan University
Kalamazoo, Michigan
December 1987**

**KINETICS OF THE METAL-EXCHANGE REACTION BETWEEN
N-(2-PYRIDYLMETHYL)IMINODIACETATONICKEL(II)
AND COPPER(II)**

Kassahun W. Beyene, M.A.

Western Michigan University, 1987

The reaction between N-(2-pyridylmethyl)iminodiacetatonickel(II), (NiPyIDA), and copper(II) was studied spectrophotometrically over the range of pH 2.30 to pH 3.30 and a 10-fold variation in copper concentration at an ionic strength of 1.25 M, and a temperature of $25.0 \pm 0.1^\circ\text{C}$. The reaction is first order in both NiPyIDA and copper (II). The reaction is pH sensitive, and terms involving proton attack and a copper dependent dissociation of the nickel complex were resolved from the data. The kinetic data are consistent with an exchange reaction which proceeds through a dinuclear intermediate having a 2-aminomethylpyridyl segment bonded to nickel and an acetate bonded to copper with the second acetate arm uncoordinated. The rate-determining step involves the rupture of the nickel-aliphatic nitrogen bond in the dinuclear intermediate. Evidence is given for a postulated mechanism of unwrapping PyIDA from the nickel complex, followed by copper attack to give a dinuclear intermediate.

A comparison of the present system to analogous metal-exchange reactions with copper(II) is made and used to account for the important kinetic features of the reaction which involve the absence of an order shift in the copper concentration as the copper concentration is increased.

ACKNOWLEDGEMENTS

The author wishes to extend his gratitude to his supervisor, Dr. Ralph K. Steinhaus, for his valuable guidance, encouragement and cooperation at all times. Sincere thanks are also given to the members of the advising committee, Dr. Dean W. Cooke and Dr. James A. Howell, for their valuable suggestions.

The financial support provided by the Department of Chemistry through a teaching assistantship is greatly appreciated. Thanks also go to Lindsey Foote for his constant encouragement .

Kassahun W. Beyene

INFORMATION TO USERS

This reproduction was made from a copy of a document sent to us for microfilming. While the most advanced technology has been used to photograph and reproduce this document, the quality of the reproduction is heavily dependent upon the quality of the material submitted.

The following explanation of techniques is provided to help clarify markings or notations which may appear on this reproduction.

1. The sign or "target" for pages apparently lacking from the document photographed is "Missing Page(s)". If it was possible to obtain the missing page(s) or section, they are spliced into the film along with adjacent pages. This may have necessitated cutting through an image and duplicating adjacent pages to assure complete continuity.
2. When an image on the film is obliterated with a round black mark, it is an indication of either blurred copy because of movement during exposure, duplicate copy, or copyrighted materials that should not have been filmed. For blurred pages, a good image of the page can be found in the adjacent frame. If copyrighted materials were deleted, a target note will appear listing the pages in the adjacent frame.
3. When a map, drawing or chart, etc., is part of the material being photographed, a definite method of "sectioning" the material has been followed. It is customary to begin filming at the upper left hand corner of a large sheet and to continue from left to right in equal sections with small overlaps. If necessary, sectioning is continued again—beginning below the first row and continuing on until complete.
4. For illustrations that cannot be satisfactorily reproduced by xerographic means, photographic prints can be purchased at additional cost and inserted into your xerographic copy. These prints are available upon request from the Dissertations Customer Services Department.
5. Some pages in any document may have indistinct print. In all cases the best available copy has been filmed.

**University
Microfilms
International**

300 N. Zeeb Road
Ann Arbor, MI 48106

Order Number 1332403

**Kinetics of the metal-exchange reaction between N-(2-pyridylmethyl)
iminodiacetatonickel(II) and Copper(II)**

Beyene, Kassahun Wodajo, M.A.

Western Michigan University, 1987

U·M·I

**300 N. Zeeb Rd.
Ann Arbor, MI 48106**

TABLE OF CONTENTS

ACKNOWLEDGEMENTS.....	ii
LIST OF TABLES.....	iv
LIST OF FIGURES.....	v
INTRODUCTION.....	1
APPARATUS AND REAGENTS.....	4
Apparatus.....	4
Reagents.....	4
EXPERIMENTAL.....	10
Spectrophotometric Study of Reactants and Products.....	10
Reaction Conditions and Rates.....	10
RESULTS.....	13
Kinetic Expression for the Reaction.....	13
Resolution of Rate Constants.....	20
DISCUSSION.....	22
Comparison to Other Ni(Ligand)-Cu Exchange Reactions.....	32
APPENDICES.....	35
A. Infra Red Spectrum of PyIDA.....	36
B. H-NMR Spectrum of PyIDA.....	39
C. Molar Absorptivity as a Function of Wavelength for CuPyIDA, Cu(II), NiPyIDA, Ni(II).....	41
D. Concentration and Absorbance Relationships.....	44
REFERENCES.....	47

LIST OF TABLES

1. Nickel Ligand Complex, Abbreviations and Ligand Structures	3
2. Molar Absorptivities of Reactants and Products at 740 nm	11
3. Experimental Conditions	12
4. Values of k_0 As a Function of pH and Copper(II) Concentration	16
5. Resolved Rate Constants for the Reaction NiPyIDA and Cu(II)	21
6. Stability and Rate Constants used in Making Comparisons of Likely Dinuclear Intermediates	23
7. Comparison of Likely Dinuclear Intermediates, NiPyIDA-Cu, for the Exchange of NiPyIDA with Cu(II) to Known Systems	24
8. Calculated Rate Constants for NiPyIDA-Cu System	27
9. List of IR Frequencies for PyIDA	38
10. Comparison Between Observed and Expected Absorbance Values for the Exchange of NiPyIDA with Cu(II)	43

LIST OF FIGURES

1. Typical First Order Plot of k_0 at Constant Copper Concentration	15
2. Effect of Copper Concentration and pH on k_0	18
3. Effect of Hydrogen Ion Concentration on k_0	19
4. Mechanism for the Transfer of PyIDA from Ni(II) to Cu(II)	28
5. Infra Red Spectrum of PyIDA	37
6. H-NMR Spectrum for PyIDA	40
7. Molar Absorptivity as a Function of Wavelength for CuPyIDA, Cu(II), NiPyIDA and Ni(II)	42

INTRODUCTION

The exchange of multidentate ligands from one metal to another, as represented by equation 1,



has been extensively studied for a variety of metal ion and aminocarboxylate ligand combinations under different conditions, using many different methods (1, 2, 3, 4, 5, 6, 7, 8, 9, 11, 12, 13). One report dealt with an interesting type of polyamine ligand having both aliphatic and aromatic dentate sites (14). The ligand, N,N'-bis-(2-picolyl)ethylenediamine, is unusual in that the aromatic nitrogens are relatively quite acidic yet without a corresponding decrease in metal-ligand complex stability (4, 5). The log stability constant of N-(2-pyridylmethyl)iminodiacetonickel(II) is 11.22 (16, 17), while that of iminodiacetonickel (II) is 8.13 (12), indicating a certain degree of added stability due to the 2-pyridylmethyl group. Thus compared to complexes of aliphatic analog, the complexes from ligands with aromatic nitrogens are far more stable in acidic solutions (13, 15, 18, 19, 20). This makes the metal-exchange reactions possible at lower pH values. Furthermore, the replacement of aliphatic nitrogens by aromatic nitrogens has a pronounced steric effect upon formation reactions with transition metals (14) and it is of interest to see whether the same effect will manifest itself in metal exchange reactions as well.

Detailed studies have shown the mechanism of these reactions to follow the successive breaking of series of coordinate bonds from the initial metal-ligand complex, followed by a stepwise coordination to the attacking metal (1, 2, 3, 4, 5, 6, 7, 13, 21,). This process leads to the formation of a dinuclear intermediate found in all

cases, where sterically possible (4, 5, 22, 23, 24, 25), followed by breakup to form products. Depending upon the system, the position of the rate determining step is a function of pH (5, 7, 8, 10), attacking metal concentration (7, 8, 11, 12, 13), the relative stability of the intermediate metal segment (3), and the relative rate of water loss from the aquo metal complex (9). In most cases, the ratio of the rate constant of the two metal-exchange systems can be approximated by the ratio of the relative stability constants for the dinuclear intermediates involved (2, 3, 5, 6, 8, 11, 12, 13). In a few cases, a change in the attacking metal concentration and hydrogen ion concentration caused shifts in the rate determining step (7, 8, 12).

The present study is concerned with the exchange reaction between Cu(II) and N-(2-pyridylmethyl)iminodiacetonickel(II), as shown in equation 2,

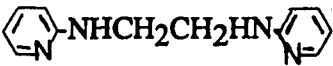



The PyIDA ligand has both aromatic and aliphatic nitrogen dentate sites in comparison to the ligands utilized in the other metal-exchange systems (3, 6, 7, 8, 10, 11, 12, 13). Ligand structures are shown in Table 1.

This study demonstrates that the reaction shown in equation 2 proceeds through two pathways: (a) a hydrogen dependent pathway, and (b) a copper dependent pathway, which proceeds through a dinuclear intermediate, Ni(PyIDA)Cu, having a 2-aminomethylpyridyl segment bonded to nickel and one acetate bonded to copper, and the other acetate uncoordinated. The structure of the dinuclear intermediate has been characterized by comparison of the rate constant ratios to the relative stability constant ratios using other similar systems. Further, a kinetic scheme has been developed that accounts for the existence of such an intermediate.

Table 1

Nickel-ligand Complex, Abbreviations and Ligand Line Formulas

NiL Complex	Abbreviations	Ligand Line Formula
Ethylenediaminetetraacetato-nickelate(II)	NiEDTA ²⁻ (HOOCCH ₂) ₂ N-CH ₂ CH ₂ -N(CH ₂ COOH) ₂	
Ethylenediaminediacetato-nickel(II)	NiEDDA HOOCCH ₂ NHCH ₂ CH ₂ HNCH ₂ COOH	
Bis(iminodiacetatoamino-N,O,O') nickelate(II)	Ni(IDA) ₂ ²⁻	HN(CH ₂ COOH) ₂
Nitrilotriacetatonickelate(II)	NiNTA ⁻	N(CH ₂ COOH) ₃
Iminodiacetatonickel(II)	NiIDA	HN(CH ₂ COOH) ₂
Ethylenediamine-N,N'-dipropionato-nickel(II)	NiEDDP HOOCCH(CH ₃)-NHCH ₂ CH ₂ HN-CH(CH ₃)COOH	
N,N'-bis(2-picolyl)ethylenediamine-nickel(II)	NiBPEDA ²⁺	
N-(2-pyridylmethyl)iminodiacetato-nickel(II)	NiPyIDA	

APPARATUS AND REAGENTS

Apparatus

All spectral measurements were done on a Cary Model 14 spectrophotometer. All the kinetic measurements were made in a 10-centimeter cell on an automatic recording spectrophotometer, Model 2000, Gilford Instrument Laboratories, Inc., which used the Beckman DU as a monochromator. The cell compartment of the spectrophotometer was maintained at a constant temperature of $25.0 \pm 0.1^\circ\text{C}$ by circulation of thermostated water from a water-bath.

The spectrophotometer settings for all kinetic measurements were as follows: wavelength 740 nm, slit width varied from 0.2-0.8 mm, reciprocal dispersion, (D^{-1}), of $37 \text{ \AA} / \text{mm}$, tungsten lamp source, chart speed 5 inches per hour.

All pH measurements were made using either a Beckman Research Model 110 pH meter or an Orion research Model 801 digital pH meter, Scientific Products. A single combination electrode was used on both meters. Beckman standard buffer solutions of pH 4.01 and pH 6.86 were used to standardize the pH meter. All pH measurements were taken at $25.0 \pm 0.1^\circ\text{C}$.

Reagents

Primary Standard. Copper(II) Nitrate

Baker analyzed reagent grade copper foil, 99.6% pure, was cleaned and rinsed in dilute nitric acid. The foil was further rinsed with water and acetone, and air dried. A weighed portion was dissolved in a minimal amount of concentrated nitric acid and diluted to volume.

Nickel(II) Nitrate

Baker analyzed reagent nickel(II) nitrate, $\text{Ni}(\text{NO}_3)_2 \cdot 6\text{H}_2\text{O}$, 99.5% pure was used to make a nickel(II) nitrate solution, which was standardized by titration against a standard EDTA at pH 5.5 using acetate buffer and 0.1% aqueous NAS as the indicator.

Copper(II) Nitrate

Copper(II) nitrate, $\text{Cu}(\text{NO}_3)_2 \cdot 3\text{H}_2\text{O}$, 99.91% pure, from Mallinckrodt Chemical Works, was used to make copper(II) nitrate solution, which was standardized with standard EDTA at pH 5.5 using acetate buffer and NAS as the indicator.

Ethylenediaminetetraacetic Acid. Disodium Salt (Na_2 EDTA)

Reagent grade ethylenediaminetetraacetic acid, disodium salt, dihydrate, 99+ % pure from Aldrich Chemical Co. was used without further purification to make an EDTA solution, which was standardized by titration with the primary standard copper(II) nitrate solution at pH of 5.5 using acetate buffer NAS as the indicator.

2-Aminomethylpyridine

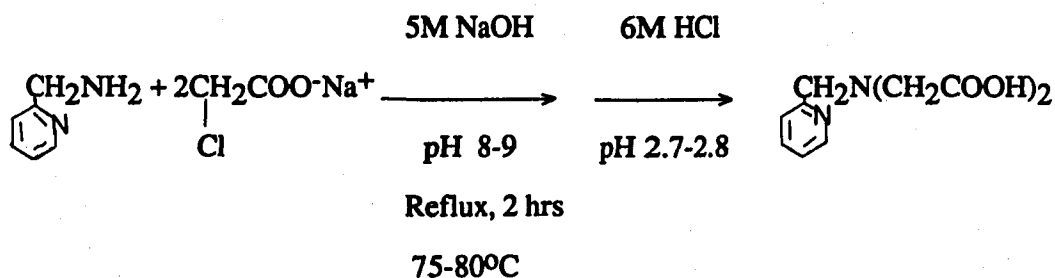
2- Aminomethylpyridine, 99% pure, from Aldrich Chemical Company, Inc. was distilled under reduced pressure (60-65 °C, 25-30 mm). The middle fraction was saved for further use.

N-(2-pyridylmethyl)iminodiacetic Acid

Condensation of 2-aminomethylpyridine and sodium monochloroacetate was used

to prepare N-(2-pyridylmethyl)iminodiacetic acid following the procedure of Irving and Da Silva (16) and Thompson (17).

The synthesis of N-(2-pyridylmethyl)iminodiacetic acid is summarized in the following scheme,



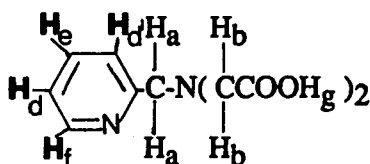
A dry, 500 mL, three-necked, round bottom flask was equipped with a Teflon - coated magnetic stirring bar, reflux condenser, and a heating mantle. The flask was charged with a solution of sodium monochloroacetate (6.99 g, 0.06 mole), dissolved in a minimum volume of water (≈ 100 mL), from which insoluble impurities were removed by filtration. Sodium monochloroacetate was obtained from Lancaster Synthesis, Ltd. Freshly distilled 2-aminomethylpyridine (3.24 g, 0.03 mole) was added dropwise from a buret over a period of 5-10 minutes. The mixture was stirred for 2 hours under reflux while maintaining the pH at about 8-9 by the dropwise addition of 5N NaOH from a buret during the period of the reflux. The tan mixture was stirred for 2 hours at a temperature between 75-80°C; chilled in an ice-salt bath (temperature, -2°C) for 2 hours and made strongly acid with 6M HCl (pH about 2.7-2.8). Then, the solution was concentrated under reduced pressure with a rotary

evaporator (15-18°C, 15-20 mm). Slight warming with an oil bath at 18-20°C allowed volume reduction at a reasonable rate. The bath was not heated above this temperature because higher temperatures caused a dark slurry material to form which makes isolation difficult. Needle shaped crystals precipitated out. More of the crystals were harvested when the solution was kept in an ice-salt bath for one day. Similar yields were obtained when the reaction mixture was allowed to cool at room temperature for over three days. The crystals were collected by suction filtration. The product was recrystallized from 95% aqueous ethanol and dried in a vacuum dessicator to constant weight. Subsequent cropping of the product was difficult because of the formation of a dark red viscous oil which upon dissolution in aqueous ethanol deposited a variety of crystals as indicated from melting point determination. No attempt was made to identify the undesired products. Recovery appeared to be unsatisfactory after the first crop. The yield of pure N-(2-pyridylmethyl)iminodiacetic acid in one crop is 2.46 g (> 37%). The m.p. was 182-183°C which is to be compared to the literature values of 174-175°C (16) and 184-18°C (17). Solutions of N-(2-pyridylmethyl) iminodiacetic acid, 0.0523g in 25 mL water-ethanol (95%), were standardized by potentiometric titration against a carbonate-free standard NaOH (0.01018 M) using a Beckman research Model 110 pH meter. Beckman standard buffer solutions, pH 4.01 and pH 6.86, were used to standardize the pH meter. The molecular weight determined from the titration was 223.4 g which is within 0.5% of the theoretical value of 224.6g. Elemental analysis gave the following : Anal. calcd. for $C_{10}H_{12}N_2O_4$: C, 53.6; H, 5.4; N, 12.5; Found : C, 51.23; H, 5.62; N, 12.22. Elemental analysis was performed by Midwest Microlab, Ltd., Indianapolis, Indiana.

The compound was analyzed for organic chlorine, to determine if traces of chloroacetic acid were present as a contaminant. Sodium fusion of the compound, followed

by the addition of acidic silver nitrate (26) showed traces of chloride to be present.

The spectral characteristics are as follows : FT IR (KBr) spectrum and the IR frequencies are shown in Figure 5 and Table 9 in the Appendix A. FT NMR (200 MHz ; D₂O) δ (ppm) : 3.61 2 protons, H_a (singlet), 4.28 4 protons, H_b (singlets), 7.51 2 protons, H_d, H_d' (multiplets), 8.02 1 proton, H_e (multiplet), 8.45 1 proton, H_f (multiplet).



H-NMR spectrum for PyIDA is shown in Figure 6 in Appendix D.

Previously reported synthesis procedures for the preparation of N-(2-pyridyl-methyl)iminodiacetic acid used an isolation method which involved forming a copper complex (16), or a rather laborious multi-operative technique (17) gives only a modest overall yield of the acid. The procedure described here was developed using a similar reaction sequence (see the scheme on page 8), and offers advantages because manipulations are simple and the procedure can be carried out in a convenient two-step operation, on a small or large scale with moderate yield. When using this procedure, it is essential to monitor the temperature and the pH of the reaction mixture. No detailed synthesis and spectral characterization of the compound has appeared in the chemical literature before .

NAS Indicator

0.1% aqueous solution was prepared using NAS,(Naphthylazone) from G. Frederick Smith Co.

Acetic Acid-Sodium Acetate Buffer

Granular sodium acetate, $\text{NaC}_2\text{H}_3\text{O}_2 \cdot 3\text{H}_2\text{O}$, analytical reagent from Mallinckodt, Inc. was used to make the acetate buffer of pH 5.5; pH adjusted to 5.5 using 6M HCl and / or 6M NaOH.

N-(2-Pyridylmethyl)iminodiacetonickel(II). (NiPyIDA)

The NiPyIDA solution was prepared by mixing equimolar volumes of nickel(II) nitrate solution and N-(2-Pyridylmethyl)iminoacetic acid. The solution was then adjusted to pH 6.5 with NaOH pellets, and the final concentration of the NiPyIDA was calculated. The concentration of NiPyIDA was also standardized spectrophotometrically after reaction with 1000 fold excess of cyanide ion at pH 10 to form the tetracyanonickelate(II) complex by comparison of the absorbance at 267 nm with that of a standard $\text{Ni}(\text{CN})_4^{2-}$ solution.

N-(2-pyridylmethyl)iminodiacetatecopper(II). (CuPyIDA)

The CuPyIDA solution was prepared by combining equimolar volumes of standard copper(II) nitrate solution with standard PyIDA followed by adjustment of pH with NaOH pellets to pH 6.5.

All solutions were prepared with deionized water that had been treated by passing distilled water through a mixed bed ion exchange column, Amberlite MB-3, and distilled twice thereafter.

All other chemicals were ACS grade and used without further purification.

EXPERIMENTAL

Spectrophotometric Study of Reactants and Products

The absorption spectra of all reactants and products were obtained from 400 nm to 800 nm. These spectra showed the largest differences in molar absorptivity between reactants and products to be at 740 nm (Figure 7 in Appendix C). All kinetic measurements were made at this wavelength. This corresponds to the absorption maximum for CuPyIDA with minimal contribution from the other species.

The molar absorptivities of all species were determined at 740 nm and are listed in Table 2. The ionic strength of all solutions was adjusted to 1.25M with 5M sodium perchlorate solution. This ionic strength was chosen in order to make comparisons of the results with previous work performed at similar ionic strengths.

Reaction Conditions and Rates

The reaction in equation 2 was studied by measuring the increase in the absorbance due to the formation of CuPyIDA. No buffer was used since there is no net change in the number of protons in the reaction . This was demonstrated by monitoring the pH as the reaction proceeded. A ten to approximately one hundred fold excess copper(II) over NiPyIDA was present in the reactions studied. The experimental conditions used in all reaction rate studies are given in Table 3.

To commence the reaction, a volume of stock copper(II) nitrate was introduced into a 150-mL beaker and enough sodium perchlorate was added to give an ionic strength of 1.25M upon dilution to the final volume. The pH was adjusted with NaOH

Table 2

Molar Absorptivities of Reactants and Products at 740 nm.¹

Species	ϵ , L mol ⁻¹ cm ⁻¹
Ni ²⁺	2.05 \pm 0.07
Cu ²⁺	9.45 \pm 0.05
CuPyIDA	71.7 \pm 0.9
NiPyIDA	3.24 \pm 0.07

¹ pH 4.00, μ = 1.25M, Temperature = 25.0 \pm 0.1°C, and Cell Path-length of 10-cm.

and / or HCl while bringing the volume to about 100 mL. The solution was transferred to a 100-mL volumetric flask and filled to the mark with deionized water. Both the copper and NiPyIDA solutions were transferred into 150-mL beakers, placed in a constant temperature bath of 25.0 \pm 0.1°C and allowed to equilibrate. At the time of the experiment, an aliquot of NiPyIDA solution, which contained 1.96×10^{-4} M NiPyIDA, was injected into the constantly stirred copper solution with a plastic syringe. The recorder to the spectrophotometer was turned on at the same time that the PyIDA solution was injected. The reaction mixture was stirred continuously for one minute, equilibrated for an additional minute, and transferred to a 10-cm spectrophotometric cell.

The reactions were monitored for at least four half-lives or approximately for four hours; however, some reactions were monitored for more than ten half-lives to

ascertain for reversibility. No evidence of a significant reverse reaction was found.

Table 3

Experimental Conditions

[NiPyIDA]	$1.96 \times 10^{-4} \text{ M}$
[Cu ⁺²]	$1.98 \times 10^{-3} \text{ M}$ to $1.98 \times 10^{-2} \text{ M}$
pH range	2.30 to 3.30 pH units
Wavelength	740 nm
Cell path length	10.0 cm
Temperature	$25.0 \pm 0.1^\circ\text{C}$
Ionic strength, μ	1.25 M

RESULTS

Kinetic Expression for the Reaction

In all rate studies the copper ion concentration was in at least a 10-fold excess over the NiPyIDA concentration. The reverse reaction was negligible under the conditions used.

The reaction of NiPyIDA with copper was found to obey the first-order rate equation

$$-d[\text{NiPyIDA}] / dt = d[\text{CuPyIDA}] / dt = k_0 [\text{NiPyIDA}] \quad (3)$$

where k_0 represents the pseudo-first-order rate constant. The integrated form of equation 3 yields,

$$\ln [\text{NiPyIDA}]_t = \ln [\text{NiPyIDA}]_0 - k_0 t \quad (4)$$

where $[\text{NiPyIDA}]_t$ is the concentration of NiPyIDA at time t , and $[\text{NiPyIDA}]_0$ is the initial concentration. The loss of NiPyIDA is inversely proportional to the formation of CuPyIDA and related to the change in absorbance as the reaction progresses.

Equation 5 relates the final absorbance, A_∞ , the absorbance at anytime time t , A_t , the molar absorptivities of reactants and products, ϵ , and the cell path-length, b , to the concentration of NiPyIDA. The derivation of equation 5 is given in Appendix D.

Plots of $-\ln (A_\infty - A_t)$ versus time were linear over four half-lives and demonstrated that the reaction in equation 3 was first-order in NiPyIDA. A typical plot is

$$[\text{NiPyIDA}] = \frac{A_t - A_\infty}{b(\epsilon_{\text{NiPyIDA}} + \epsilon_{\text{Cu}^{+2}} - \epsilon_{\text{CuPyIDA}} - \epsilon_{\text{Ni}^{+2}})} \quad (5)$$

shown in Figure 1 .

After the kinetic behavior was well established, a curve fitting program was used for each set of data to obtain optimum values of the observed pseudo-first-order rate constant, the final absorbance of the reaction, A_∞ , and the change in absorbance that the reaction experienced, A_1 . The program gave the best least-squares fit for equation 6.

$$A_t = A_1 e^{-kt} + A_\infty \quad (6)$$

Very good agreement between the predicted and experimental absorbance values was found showing that the reaction went to completion.

The order in copper obtained by monitoring reactions at constant hydrogen ion concentration in which the copper concentration was varied between a 10- and a 100-fold molar excess over NiPyIDA. Table 4 lists the data. Figure 2 demonstrates the linearity of the plots obtained from the data in Table 4.

The effect of pH variation upon the rate is shown in Figure 2, which demonstrates that the exchange reaction is pH sensitive since the rate constant increases with decreasing pH values. The pH range studied was between pH 2.30 and pH 3.30.

The dependence upon hydrogen ion concentration was established by measuring the reaction rate over at least a 10-fold excess in copper(II) concentration and varying the pH from 2.30 to 3.30. A plot of the intercept for each line shown in Figure 2 is plotted as the function of hydrogen ion concentration and Figure 3 is obtained. This is linear, thus demonstrating first-order behavior in hydrogen ion concentration.

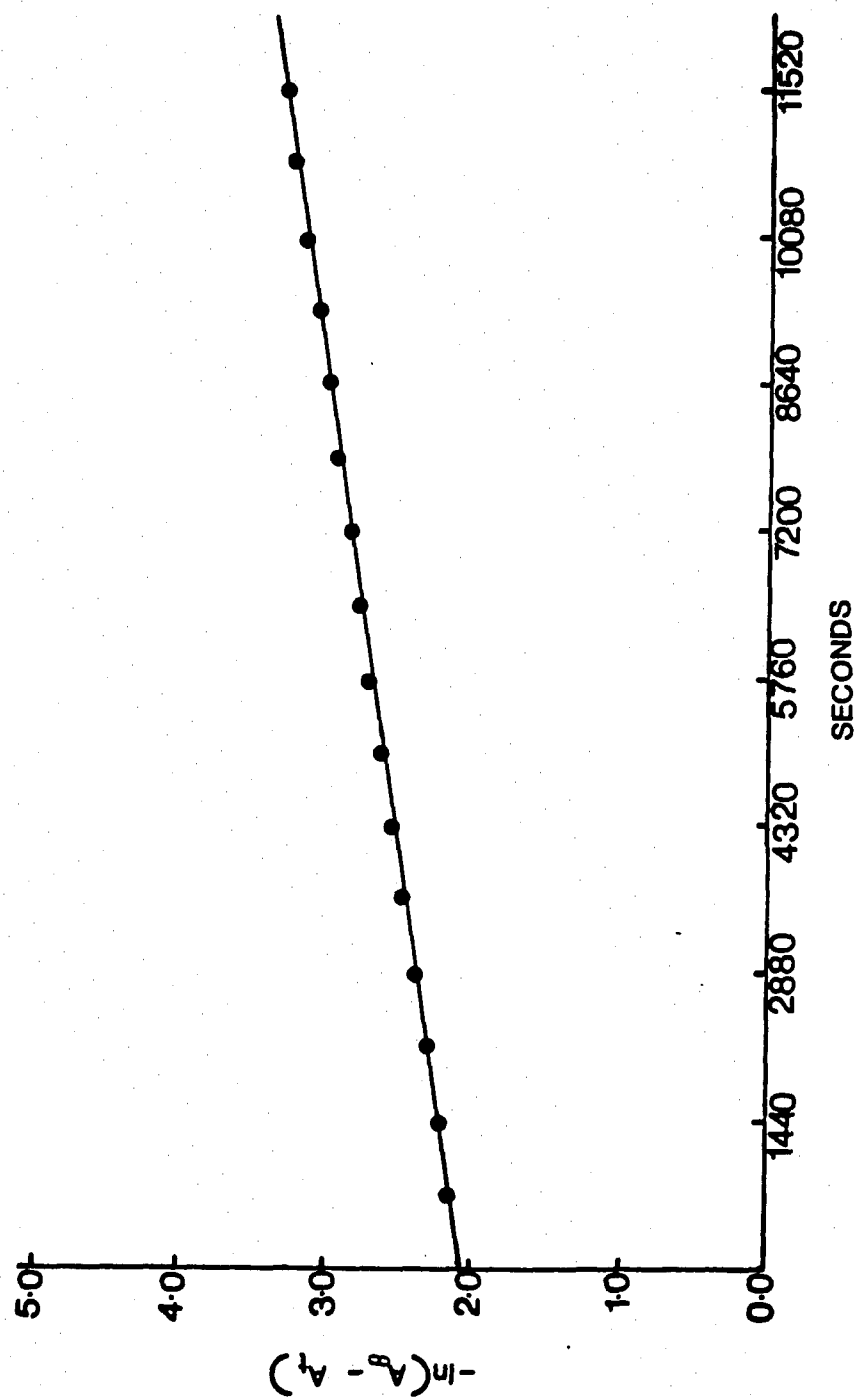


Figure 1 . Typical First Order Plot of k_0 at Constant Copper Concentration , $\mu = 1.25$. $T = 25^\circ\text{C}$.

Table 4

Values of k_O as a Function of pH and Copper(II) Ion Concentration.¹

pH	[Cu ⁺²], M	k_O , sec ⁻¹
2.30	1.98 x 10 ⁻³	(6.36 ± 0.04) x 10 ⁻⁴
	3.96 x 10 ⁻³	(6.09 ± 0.05) x 10 ⁻⁴
	5.93 x 10 ⁻³	(6.66 ± 0.06) x 10 ⁻⁴
	7.91 x 10 ⁻³	(6.79 ± 0.09) x 10 ⁻⁴
2.52	1.98 x 10 ⁻³	(6.36 ± 0.04) x 10 ⁻⁴
	3.96 x 10 ⁻³	(3.61 ± 0.04) x 10 ⁻⁴
	5.93 x 10 ⁻³	(3.98 ± 0.03) x 10 ⁻⁴
	7.91 x 10 ⁻³	(3.88 ± 0.07) x 10 ⁻⁴
2.75	1.98 x 10 ⁻³	(1.52 ± 0.08) x 10 ⁻⁴
	3.95 x 10 ⁻³	(1.68 ± 0.04) x 10 ⁻⁴
	5.93 x 10 ⁻³	(1.78 ± 0.03) x 10 ⁻⁴
	7.91 x 10 ⁻³	(1.54 ± 0.01) x 10 ⁻⁴
	9.89 x 10 ⁻³	(1.90 ± 0.01) x 10 ⁻⁴
	1.19 x 10 ⁻²	(2.08 ± 0.01) x 10 ⁻⁴
	1.58 x 10 ⁻²	(2.21 ± 0.02) x 10 ⁻⁴
	1.98 x 10 ⁻²	(2.39 ± 0.04) x 10 ⁻⁴
3.01	1.98 x 10 ⁻³	(9.28 ± 0.11) x 10 ⁻⁵
	3.96 x 10 ⁻³	(9.65 ± 0.13) x 10 ⁻⁵
	5.93 x 10 ⁻³	(9.65 ± 0.11) x 10 ⁻⁵

Table 4 --Continued

pH	[Cu ⁺²], M	k _o , sec ⁻¹
3.30	7.91 x 10 ⁻³	(9.85 ± 0.14) x 10 ⁻⁵
	1.98 x 10 ⁻³	(3.83 ± 0.05) x 10 ⁻⁵
	3.96 x 10 ⁻³	(4.01 ± 0.20) x 10 ⁻⁵
	5.93 x 10 ⁻³	(3.57 ± 0.20) x 10 ⁻⁵
	7.91 x 10 ⁻³	(7.46 ± 0.30) x 10 ⁻⁵

¹ At Constant [NiPyIDA] = 1.96 x 10⁻⁴ M. μ = 1.25 , T = 25.0 ± 0.1°C.

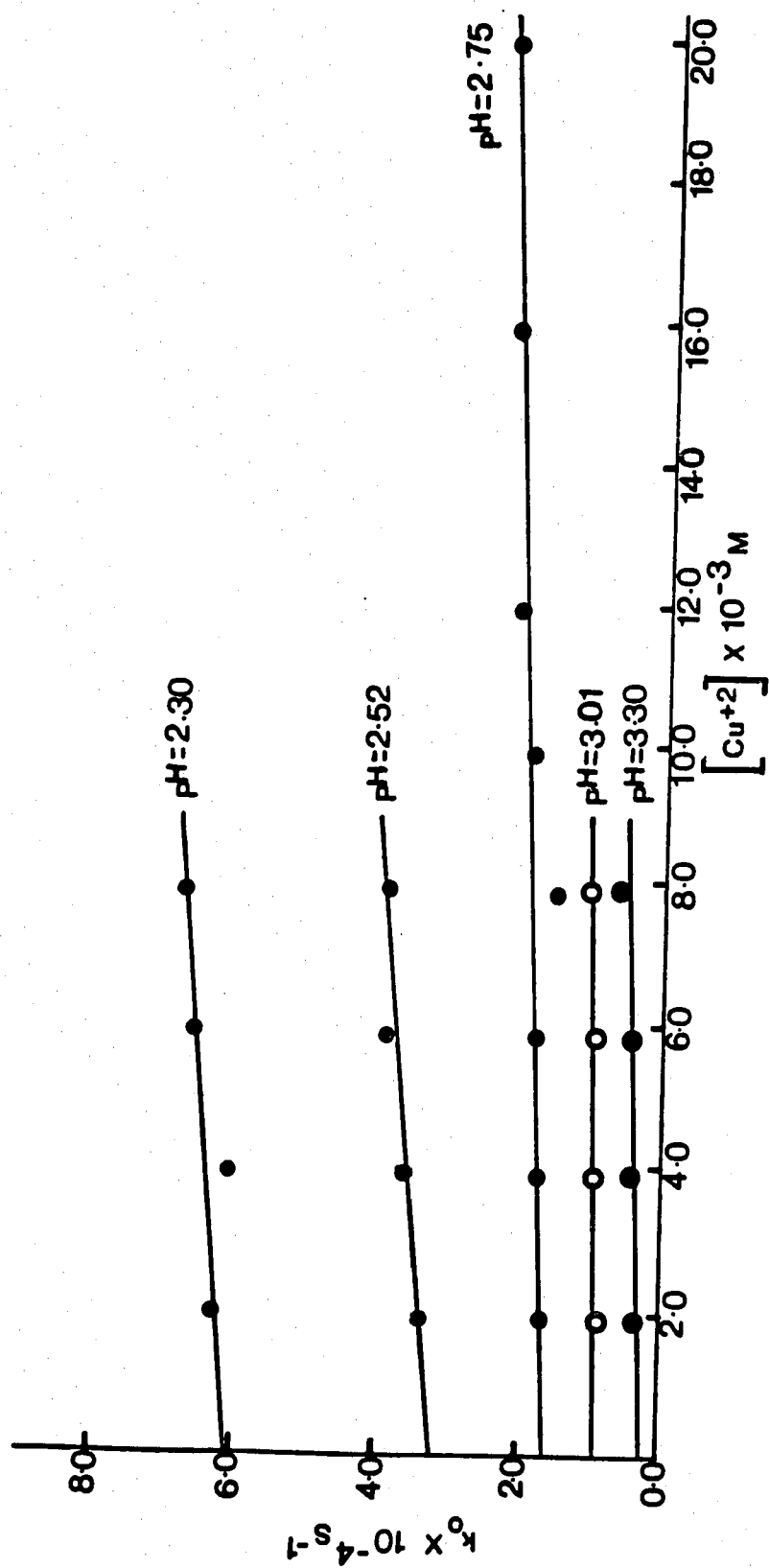


Figure 2. Effect of Copper Concentration and pH on k_o ($\mu = 1.25$, $T = 25^\circ\text{C}$).

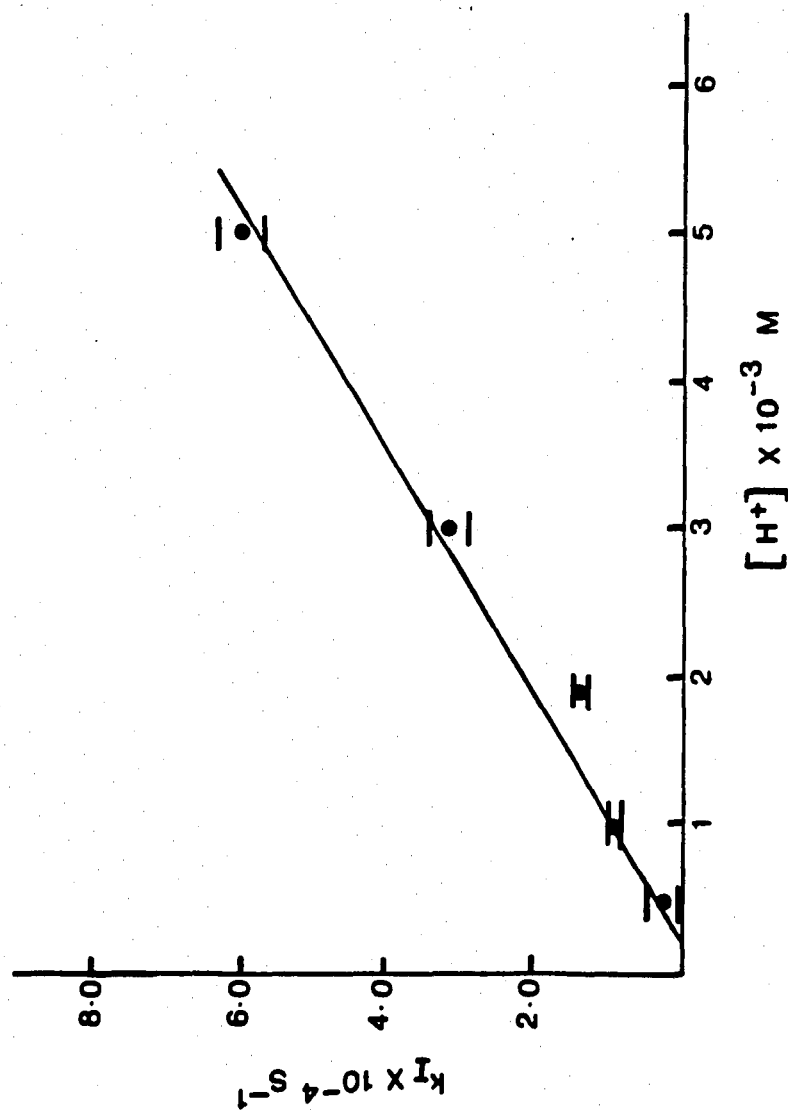


Figure 3. Effect of Hydrogen Ion Concentration on k_I . $\mu \approx 1.25$. $T = 25^\circ\text{C}$.

Resolution of Rate Constants

The effect that the change in copper concentration has on k_0 is shown in Figure 2, at several pH values. A linear dependence was found throughout the entire copper concentration range studied analogous to the NiEDDP-Cu (13), NiIDA-Cu (11) and NiHEEDTA-Cu (26) systems . This is in marked contrast to the NiEDTA-Cu (7), NiEDDA-Cu (8) and Ni(IDA)₂²⁻- Cu (12) systems which showed a variation in order with respect to copper concentration as the copper concentration was increased. The value of the copper dependent term, $k_{Cu}^{NiPyIDA}$, was obtained from the slopes of the lines at constant pH shown in Figure 2. The average value of $k_{Cu}^{NiPyIDA}$, obtained from the linear least-squares analysis of the data in Table 4 is $(6.23 \pm 0.22) \times 10^{-3} \text{ M}^{-1}\text{S}^{-1}$. The intercept of these plots is a hydrogen dependent term for the dissociation of NiPyIDA.

Values of the intercepts, k_I , of the lines shown in Figure 2, are copper independent terms for each pH studied. A plot of k_I versus hydrogen ion concentration shown in Figure 3 was linear. The slope of this line represents the hydrogen dependent term, $k_H^{NiPyIDA}$. The value obtained from the least-squares analysis for $k_H^{NiPyIDA}$ is $(1.28 \pm 0.06) \times 10^{-1} \text{ M}^{-1}\text{S}^{-1}$. The intercept was a small negative number, $k_I = (-5.34 \pm 2.01) \times 10^{-5} \text{ S}^{-1}$, which indicates that the copper and hydrogen independent dissociation of NiPyIDA is negligible or non-observable under the experimental conditions studied. Similar conclusions were arrived at in other studies (11, 13) for copper-independent and hydrogen-independent pathway. The resolved rate constants are listed in Table 5.

Previous studies on similar systems (7, 8, 9, 10, 11, 12, 13) have shown the following terms to contribute to the rate of metal-exchange reaction: Proton attack, copper attack, and pH and copper-independent dissociation of the initial nickel

complex. Each of these play a large or small role or may be non-observable in a given metal-exchange system depending upon the ligand and metal pair involved.

A complete rate equation for metal-exchange, showing all possible terms, is given in equation 7.

$$-d[\text{NiPyIDA}]/dt = (k_{\text{Cu}}^{\text{NiPyIDA}} [\text{Cu}^{+2}] + k_{\text{H}}^{\text{NiPyIDA}} [\text{H}^+] + k^{\text{NiPyIDA}} [\text{NiPyIDA}]) \quad (7)$$

Since the term k^{NiPyIDA} is experimentally not observed, equation 7 can be expressed as shown in equation 8 for the system under study.

$$-d[\text{NiPyIDA}]/dt = (k_{\text{Cu}}^{\text{NiPyIDA}} [\text{Cu}^{+2}] + k_{\text{H}}^{\text{NiPyIDA}} [\text{H}^+]) [\text{NiPyIDA}] \quad (8)$$

where $k_o = k_{\text{Cu}}^{\text{NiPyIDA}} [\text{Cu}^{+2}] + k_{\text{H}}^{\text{NiPyIDA}} [\text{H}^+]$.

Table 5

The Resolved Rate Constants for the Reaction of NiPyIDA and Copper

Constants	Values
$k_{\text{H}}^{\text{NiPyIDA}}$	$(1.28 \pm 0.06) \times 10^{-1} \text{ M}^{-1}\text{S}^{-1}$
$k_{\text{Cu}}^{\text{NiPyIDA}}$	$(6.23 \pm 0.22) \times 10^{-3} \text{ M}^{-1}\text{S}^{-1}$

$^1\mu = 1.25 \text{ M}$, $T = 25.0 \pm 0.1^\circ\text{C}$.

DISCUSSION

The NiPyIDA-Cu(II) reaction appears to proceed through two different pathways :
 (a) a proton-assisted dissociation of NiPyIDA followed by attack of copper(II) ion on the dissociated ligand, the pathway represented by k_H^{NiPyIDA} , and (b) an attack by copper(II) ion on partially unwrapped NiPyIDA to yield a dinuclear intermediate, the pathway represented by $k_{\text{Cu}}^{\text{NiPyIDA}}$.

The structure of the dinuclear intermediate may be obtained using the same procedures followed for other similar systems (3, 4, 5, 8, 11, 12, 13). Previous metal-exchange studies have shown that the structure of the dinuclear intermediate immediately prior to the rate-determining step may be characterized by comparison of the rate constant ratios involving similar systems to the relative stability constant ratios for the same system as shown in equation 9.

$$\frac{k_{\text{Cu}}^{\text{NiPyIDA}}}{k_{\text{Cu}}^{\text{NiL}}} = \frac{K_r^{\text{Ni(PyIDA)Cu}}}{K_r^{\text{Ni(L)Cu}}} \quad (9)$$

The comparison assumes the rate-determining step to hold for both systems. The values of K_r is calculated according to equation 10 where $K_{\text{Ni segment}}$ and $K_{\text{Cu segment}}$ are the stability constants of that portion of the ligand bonded to nickel and copper respectively and $K_{\text{Ni complex}}$ is the stability constant of the original nickel ligand. The values of K_r were calculated from known stability constants listed in Table 6 chosen to be as consistent as possible with respect to temperature and ionic strength. Table 7 lists the comparison between the known structures and the seven

Table 6


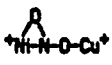
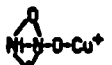
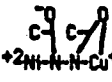
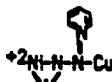
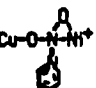
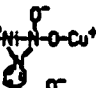
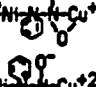
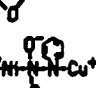
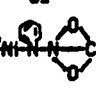
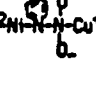
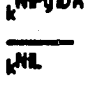
Stability and Rate Constants used in Making Comparisons of Likely
Dinuclear Intermediates.^a

Complex	K _{stab}	M	k _{Cu^{Ni}L} , M ⁻¹ s ⁻¹
NiPyIDA	1.66 x 10 ¹¹	Cu	6.23 x 10 ⁻³ b
NiEDDP	1.58 x 10 ¹²	Cu	7.51 x 10 ⁻³ c
NiEDDA	4.46 x 10 ¹³	Cu	7.49 x 10 ⁻³ d
NiEDTA ²⁻	3.31 x 10 ¹⁸	Cu	1.6 x 10 ⁻² e
NiHEEDTA ⁻	1.25 x 10 ¹⁷	Cu	1.5 x 10 ⁻² f
NiNTA ⁻	3.16 x 10 ¹¹	Cu	1.3 x 10 ⁻³ g
NiIDA	1.34 x 10 ⁸	Cu	1.48 x 10 ⁻² h
NiBPEDA ²⁺	2.51 x 10 ¹⁴	Cu	4.9 x 10 ⁻⁴ i
Intermediate metal segment			
Ni(glycinate) ⁺	1.95 x 10 ⁵		
Ni(NH ₃) ⁺²	5.01 x 10 ²		
Ni(acetate) ⁺	5.5		
Ni(pyridine) ⁺²	6.31 x 10 ¹		
Ni(2-aminomethylpyridine) ⁺²	1.26 x 10 ⁷		
Ni(N-(2-pyridylmethyl)glycinate) ⁺	1.58 x 10 ¹⁰		
Cu(glycinate) ⁺	3.63 x 10 ⁷		
Cu(NH ₃) ⁺²	1.99 x 10 ⁴		
Cu(acetate) ⁺	5.25 x 10 ¹		
Cu(pyridine) ⁺²	2.51 x 10 ²		
Cu(IDA)	1.23 x 10 ¹¹		
Cu(2-aminomethylpyridine) ⁺²	3.16 x 10 ⁹		
Cu(N-(2-pyridylmethyl)glycinate) ⁺	6.31 x 10 ¹¹		

^a all values are either at 25 °C and $\mu = 0.1\text{M}$ or chosen to be as close to these conditions as possible. Except as noted all values are taken from reference 28, 29, 30, 31. ^bThis work. ^creference 13. ^dreference 1, 8. ^ereference 7. ^freference 3. ^greference 5. ^hreference 12. ⁱreference 11.

Table 7

Comparison of Likely Dinuclear Intermediates, NiPyIDA-Cu for the Exchange of NiPyIDA with Cu (II) to Known Systems.^a

						
Ni (EDDA) Cu $K_F=1.91$	Ni (IDA) Cu $K_F=0.244$	Ni (NTA) Cu $K_F=0.022$	NiKEDDP) Cu $K_F=0.0428$ $K_{01}=10^6$	Ni (BPEDA) Cu $K_F=0.0012$		
STRUCTURES to be Tested	K_F	$K_F \text{Ni(PyIDA)Cu} / K_F \text{Ni(EDDA)Cu}$	$K_F \text{Ni(PyIDA)Cu} / K_F \text{Ni(IDA)Cu}$	$K_F \text{Ni(PyIDA)Cu} / K_F \text{Ni(NTA)Cu}$	$K_F \text{Ni(PyIDA)Cu} / K_F \text{NiKEDDP)Cu}$	$K_F \text{Ni(PyIDA)Cu} / K_F \text{Ni(BPEDA)Cu}$
I. 	6.17×10^{-5}	3.23×10^{-5}	2.52×10^{-4}	$5.91 \times 10^{-3}^{b,d}$	1.44×10^{-3}	0.162^b
II. 	3.98×10^{-3}	$6.56 \times 10^{-2}^o$	0.513^c	$3.798^{c,d}$	0.293^c	104.5^c
III. 	1.38×10^{-2}	$2.28 \times 10^{-2}^b$	0.178^b	$1.32^{b,d}$	1.02^b	36.3^b
IV. 	2.95×10^{-4}	$4.88 \times 10^{-4}^b$	$3.82 \times 10^{-3}^b$	$2.92 \times 10^{-2}^{b,d}$	$2.18 \times 10^{-2}^b$	0.777^b
V. 	7.58×10^{-7}	$1.25 \times 10^{-6}^b$	$9.82 \times 10^{-6}^b$	$1.09 \times 10^{-4}^b$	$5.59 \times 10^{-5}^b$	$1.99 \times 10^{-3}^b$
VI. 	46.8	24.5	191.8	2127	109.3^e	39000
VII. 	7.56×10^{-6}	$1.25 \times 10^{-5}^b$	$9.79 \times 10^{-5}^b$	$1.08 \times 10^{-3}^b$	$5.58 \times 10^{-4}^b$	$1.99 \times 10^{-2}^b$
$\frac{k_{\text{NiPyIDA}}}{k_{\text{NiL}}}$		8.20×10^{-2}	0.421	4.79	0.828	12.7

^a K_F values are based on the stability constants given in Table 6 and chosen to be as internally consistent as possible with respect to temperature and ionic strength. The experimental ratios of rate constants are based upon the rate constants given in Table 6, with $\mu = 1.25\text{M}$, $T = 25^\circ\text{C}$. ^b Electrostatic factor 3.15. ^c Electrostatic of 31.5 included. ^d Statistical factor of 2/3 included. ^e Reference 15.

logical dinuclear intermediate structures for NiPyIDA-Cu.

$$K_T = \frac{K_{\text{Ni segment}} \times K_{\text{Cu segment}}}{K_{\text{Ni complex}}} \quad (10)$$

In some comparisons an electrostatic attraction helps stabilize one intermediate relative to the other (13, 27). The added stability of this contribution is an electrostatic factor, K_{el} , and can be estimated using equation 11 in Bydelek and Margerum (4).

$$\log K_{el} = \frac{Z_A Z_B e^2}{2.303 R T \epsilon_{rAB}} \quad (11)$$

Where Z_A and Z_B the charges involved, e is the charge, ϵ is the dielectric constant of water, r_{AB} is the charge separation estimated from molecular models, T is temperature in Kelvin, and R is the gas constant.

There may also be a statistical factor which favors the formation of one intermediate over another and this term must be included in making comparisons.

Values of K_{el} and statistical factors are included where appropriate. The last row in Table 7 shows the ratios of experimental rate constants. A comparison of the ratio of experimental rate constants to the predicted ratios of intermediate stability constants shows that structures II and III give values which agree closely to the experimental rate constant ratios. Other structures listed in Table 6 and as well as some not listed were tested and gave values which differ by several orders of magnitude.

In order to determine which of the two structures, II or III, is the dinuclear intermediate, the value of $k_{CuNiPyIDA}$ is estimated for each and compared to the experimental value of $6.23 \times 10^{-3} \text{ M}^{-1}\text{S}^{-1}$. As shown in equation 12 the value of

$k_{\text{Cu}}^{\text{NiPyIDA}}$ can be estimated from the relative stability constant of species II or III, an estimate of the value of the rate - determining step, k_{rds} , for that species and any appropriate electrostatic factor .

$$k_{\text{Cu}}^{\text{NiPyIDA}} = K_r k_{\text{rds}} k_{\text{el}} \quad (12)$$

Structure II has both an aliphatic nitrogen and an aromatic nitrogen bonded to nickel. The rate - determining step will be the slower of the two cleavages. Since nickel - aromatic bonds cleave at 38.5 S^{-1} (14) and nickel-aliphatic nitrogen bonds cleave at 0.3 S^{-1} , (11, 27), the rate - determining step would seem to be the nickel-aliphatic bond cleavage. Structure III involves breakage of the nickel aromatic-nitrogen bond as the rate - determining step. These bonds cleave at 38.5 S^{-1} (14).

Species II involves an electrostatic factor of 31.5 while that for species III is 3.15. Thus the predicted values of $k_{\text{Cu}}^{\text{NiPyIDA}}$ are $3.76 \times 10^{-3} \text{ M}^{-1}\text{S}^{-1}$ for species II and $1.67 \text{ M}^{-1} \text{ S}^{-1}$ for species III . Comparison to the experimental value of $6.23 \times 10^{-3} \text{ M}^{-1} \text{ S}^{-1}$ shows species II to give a value only a factor of 2 lower than the experimental value, whereas species III gives a value 268 times greater than the experimental value. This suggests that species II as the likely dinuclear intermediate.

A similar estimation can be made for the value of $k_{\text{H}}^{\text{NiPyIDA}}$, the proton dependent dissociation, assuming species II to be correct . Equation 12 is again used. The value of K_r is calculated from equation 10 with K_{H} -segment in place of K_{Cu} -segment . The value of $\text{pK}_{\text{a}1}$ for glycine = 2.36 (30, 31) is used to calculate K_{H} -segment . There is also an electrostatic factor of 31.5 . Thus, K_r is 1.74×10^{-2} and equation 12 gives $k_{\text{H}}^{\text{NiPyIDA}} = 1.64 \times 10^{-1} \text{ M}^{-1}\text{S}^{-1}$ for species II which compares favorably with the experimental value of $1.28 \times 10^{-1} \text{ M}^{-1}\text{S}^{-1}$. The calculated $k_{\text{H}}^{\text{NiPyIDA}}$ value for species III is $2.11 \text{ M}^{-1} \text{ S}^{-1}$ which is 13 times

larger than the experimental value. The estimated and experimental values of both $k_{\text{Cu}}^{\text{NiPyIDA}}$ and $k_{\text{H}}^{\text{NiPyIDA}}$ are shown in Table 8.

Table 8

Calculated Rate Constants for NiPyIDA-Cu System

	Calculated	Experimental
$K_{\text{Cu}}^{\text{NiPyIDA}}$	$3.76 \times 10^{-3} \text{M}^{-1} \text{S}^{-1}$	$(6.23 \pm 0.22) \times 10^{-3} \text{M}^{-1} \text{S}^{-1}$
$K_{\text{H}}^{\text{NiPyIDA}}$	$1.64 \times 10^{-1} \text{M}^{-1} \text{S}^{-1}$	$(1.28 \pm 0.06) \times 10^{-1} \text{M}^{-1} \text{S}^{-1}$

A mechanism which is consistent with the results obtained for the exchange reaction is presented in Figure 4. Protons are omitted from the mechanism for simplicity although step 1 \rightarrow 2 is proton dependent. Further, the sequence 1 \rightarrow 2 \rightarrow 3 \rightarrow 5 will be shown to be negligible.

The copper dependent exchange pathway in Figure 4 is 1 \rightarrow 2 \rightarrow 4 \rightarrow 5. Step 2 \rightarrow 4 should not be rate-limiting since it involves reaction of the labile aquo- copper ion which has a rate of water loss of $3 \times 10^8 \text{S}^{-1}$ (32). Step 1 \rightarrow 2 could not be rate limiting because it would result in zero-order behavior in copper for all the pathways of the exchange. This leaves step 4 \rightarrow 5 as the rate-limiting step for copper dependent pathway, $k_{\text{Cu}}^{\text{NiPyIDA}}$.

The reaction paths 1 \rightarrow 2 \rightarrow 4 \rightarrow 5 and 1 \rightarrow 2 \rightarrow 3 \rightarrow 5 both contribute to the formation of products. The latter reaction path, however, is controlled by the rate of

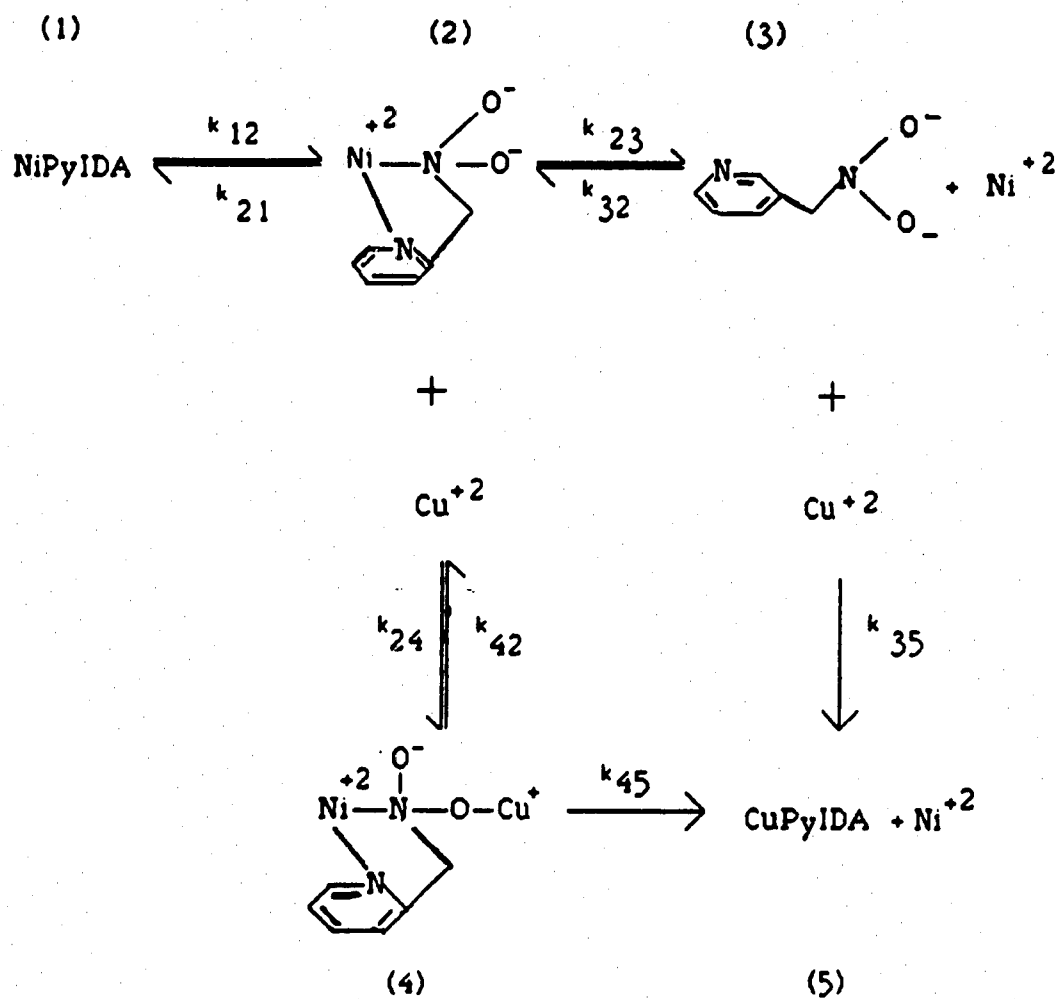


Figure 4. Mechanism of Transfer of PyIDA from Ni^{+2} to Cu^{+2} .

dissociation of NiPyIDA, and is not dependent on copper or hydrogen ion concentration and was experimentally shown to be negligible in the present study.

The reaction sequence 1 \rightarrow 2 \rightarrow 4 \rightarrow 5 of Figure 4 is represented by $k_{\text{Cu}}^{\text{NiPyIDA}}$ and $k_{\text{H}}^{\text{NiPyIDA}}$, and a general kinetic expression can be derived from it, as shown in equation 13.

$$-d[\text{NiPyIDA}]/dt = d[\text{CuPyIDA}]/dt = k_0 [\text{NiPyIDA}] = k_{45} [\text{Species 4}] \quad (13)$$

Assuming the steady-state approximation for species 2 and 4 yields expression 14 and 15 where X refers to either copper ion or hydrogen ion.

$$[2] = \frac{k_{12}[1] + k_{42}[4]}{k_{24} + k_{24}[X]} \quad (14)$$

$$[4] = \frac{k_{24}[2][X]}{k_{42} + k_{45}} \quad (15)$$

Substituting equation 14 into equation 15 gives expression 16,

$$[4] = \frac{k_{12} k_{24} [1][X]}{k_{21} k_{42} + k_{21} k_{45} + k_{24} k_{45} [X]} \quad (16)$$

and substitution of expression 16 into the general rate expression, equation 13, yields equation 17.

$$d[\text{NiPyIDA}]/dt = \frac{k_{12}k_{24}k_{45}[1][X]}{k_{21}k_{42} + k_{21}k_{45} + k_{24}k_{45}[X]} \quad (17)$$

$$\text{where, } k_o = \frac{k_{12}k_{24}k_{45}[X]}{k_{21}k_{42} + k_{21}k_{45} + k_{24}k_{45}[X]} \quad (18)$$

A comparison of the terms in the denominator of equation 18 allows some simplification of the expression. The term $k_{24}k_{45}[X] > k_{21}k_{45}$ because k_{24}/k_{21} is at least 10^4 due to the difference in rate of water loss between copper and nickel and the fact that (a) the largest of the two, copper or hydrogen ion, predominates kinetically and (b) either the copper or hydrogen ion concentration is always at least 2.0×10^{-3} M or greater. Further, the term $k_{21}k_{42} \gg k_{24}k_{45}[X]$ because the dissociation of copper acetate, k_{42} , is about 10^8 greater than the dissociation of nickel-amine, k_{45} , but $k_{24}[X]$ is only about 10 times greater than k_{21} due to the difference in copper and nickel water loss rates and the lower limit on $[X]$. Thus, $k_{21}k_{42}$ predominates in the denominator such that equation 18 simplifies to equation 19, which shows the first-order dependence in copper and hydrogen ion concentration that was found experimentally.

$$k_o = \frac{k_{12}k_{24}k_{45}[X]}{k_{21}k_{42}} \quad (19)$$

The first-order dependence in copper and hydrogen described in equation 19 was

found to hold over the entire range of copper and hydrogen ion concentration studied.

Likewise, a kinetic expression may be derived for the pathway $1 \rightarrow 2 \rightarrow 3 \rightarrow 5$ by assuming a steady-state for species 2. The expression is given in equation 20.

$$k_{\text{NiPyIDA}} = \frac{k_{12}k_{23}}{k_{21} + k_{23}} \quad (20)$$

In the denominator of equation 20, k_{21} , which represents nickel-acetate bond formation, is much greater than k_{23} which represents nickel-aliphatic nitrogen bond dissociation. Thus, equation 20 simplifies to give equation 21 with k_{23} as the rate determining step.

$$K_{\text{NiPyIDA}} = \frac{k_{12}k_{23}}{k_{21}} \quad (21)$$

The contribution from the exchange sequence $1 \rightarrow 2 \rightarrow 3 \rightarrow 5$ is minimal as the following calculations show. The rate of dissociation NiPyIDA, k_{diss} , can be calculated according to equation 22 from the stability constant and predicted rate of formation of the complex. The stability constant of NiPyIDA is 1.66×10^{11} . The rate of formation may be estimated (33) from K_{OS} , outer sphere association, and $k_{-\text{H}_2\text{O}}$, the rate of water loss of nickel.

$$K_{\text{stab}} = \frac{K_{\text{OS}} k_{-\text{H}_2\text{O}}}{k_{\text{diss}}} \quad (22)$$

K_{OS} has been calculated to be 20 M^{-1} for the reaction of species whose charges are

+2, nickel, and -2, PyIDA (33). The distance of closest approach has been estimated to be 4 \AA for an acetate arm . The rate of water loss of $\text{Ni}(\text{H}_2\text{O})_6^{+2}$ is $2.7 \times 10^4 \text{ S}^{-1}$ (33). Equation 22, using the above values, gives k_{diss} of NiPyIDA to be $3 \times 10^{-6} \text{ S}^{-1}$ which is two thousand times lower than the contribution from the reaction path $1 \rightarrow 2 \rightarrow 4 \rightarrow 5$, thus explaining why k_{diss} of NiPyIDA was not observed experimentally .

Comparison to Other Ni(Ligand)-Cu Exchange Reactions

All Ni(ligand)-Cu metal exchange reactions are found to proceed through a dinuclear intermediate except where there is a large steric hinderance (2, 23, 25) and the attacking metal cannot kinetically participate in the replacement of another metal in a metal-complex. Some show a shift in order with respect to copper from first-order in copper at low copper concentration to zero-order in copper at high copper concentration. The copper exchange with NiEDDA (8), NiEDTA^{2-} (7) and Ni(IDA)_2^{2-} (12, 27) all exhibit this behavior. Other Ni(ligand)-Cu exchange reactions show only first-order behavior in copper for the entire copper concentration range studied. Systems involving NiIDA (12, 26) NiBPEDA^{2+} (11), NiEDDP (13, 25), NiHEEDTA^- (3) and NiPyIDA (this work) show this behavior.

The order of the reaction with respect to copper depends upon the value of [species 4] k_{45} . The concentration of species 4 relative to species 2 is given in equation 23 using the steady state approximation in the general mechanism in Figure 4. As the copper concentration in the solution increases, equation 23 shows that the relative concentration of species 4 increases, and the rate increases.

$$\frac{[4]}{[2]} = \frac{k_{24} [Cu^{+2}]}{k_{42} + k_{45}} \quad (23)$$

Equation 23 also provides the key to understanding why certain exchange systems show order shift and others do not exhibit this kinetic behavior.

In the reaction of copper with NiIDA, NiEDDP, NiBPEDA²⁺ and NiPyIDA, and NiEDDA, NiEDTA²⁻ and Ni(IDA)₂²⁻, k_{24} and k_{45} are essentially the same, copper rate of water loss and nickel-nitrogen bond dissociation, respectively. Thus the value of k_{42} is important in determining the relative size of [species 4]. The structure of the dinuclear intermediate actually determines the value k_{42} since the extent of unwrapping and subsequent coordination to copper determines what segment must dissociate from copper in step 4--->2. Dinuclear intermediates where very little ligand has unwrapped or where copper does not fully bond to the unwrapped segment will have large values of k_{42} approximately 10^6 and 10^4 S⁻¹ (12) which is much larger than k_{45} . Therefore the relative concentration of species 4 will be small. The k_{42} values are approximated from the rate of water loss of copper, 3×10^8 S⁻¹ (34), and the relative stability constant of the ligand segment bonded to copper. When a large portion of the ligand has unwrapped, smaller values of k_{42} results. The NiEDDA, NiEDTA²⁻ and Ni(IDA)₂²⁻ systems represent this class and have k_{42} values of approximately 10 S⁻¹ (12), 10^{-3} S⁻¹ (12), and 10^{-3} S⁻¹ (34), respectively which are similar to or less than k_{45} so that the relative concentration of species 4 will be large. Thus, the relative concentration of species 4 will be considerably larger for the NiEDDA, NiEDTA²⁻ and Ni(IDA)₂²⁻ systems than NiIDA, NiBPEDA²⁺, NiEDDP and NiPyIDA system. For a given system with a large portion of the ligand unwrapped, both k_{12} and k_{42} will be

small so that an increase in copper concentration can cause (a) the relative concentration of species 4 to increase, and (b) $[4] k_{45}$ to exceed k_{12} , thus making k_{12} rate limiting. The rate limiting step shifts from step 4 \rightarrow 5 to step 1 \rightarrow 2 as a function of copper concentration.

Experimentally, no order shift was seen in the NiPyIDA-Cu system. Since only an acetate group is bonded to copper, both k_{12} and k_{42} must be quite large. Thus the relative concentration of species 4 is small and the increase in copper concentration is not enough to cause $[4] k_{45} > k_{12}$, resulting in first-order behavior in copper over the entire copper concentration range.

The general conclusion has been drawn earlier (12, 13) and again from this study that systems in which the dinuclear intermediate occurs early in the unwrapping process with the correspondingly large values k_{12} and a large value of k_{42} will not show an order shift as the concentration of the attacking metal is increased. The same conclusion can be reached if the attacking metal does not fully bond to the unwrapped ligand since this will cause k_{42} to be large despite the fact the k_{12} may be small. However, if large portions of the ligand unwrap and bond to the attacking metal prior to the rate determining step, a shift in order with respect to the attacking metal can be expected.

APPENDICES

Appendix A

Infra Red Spectrum of PyIDA

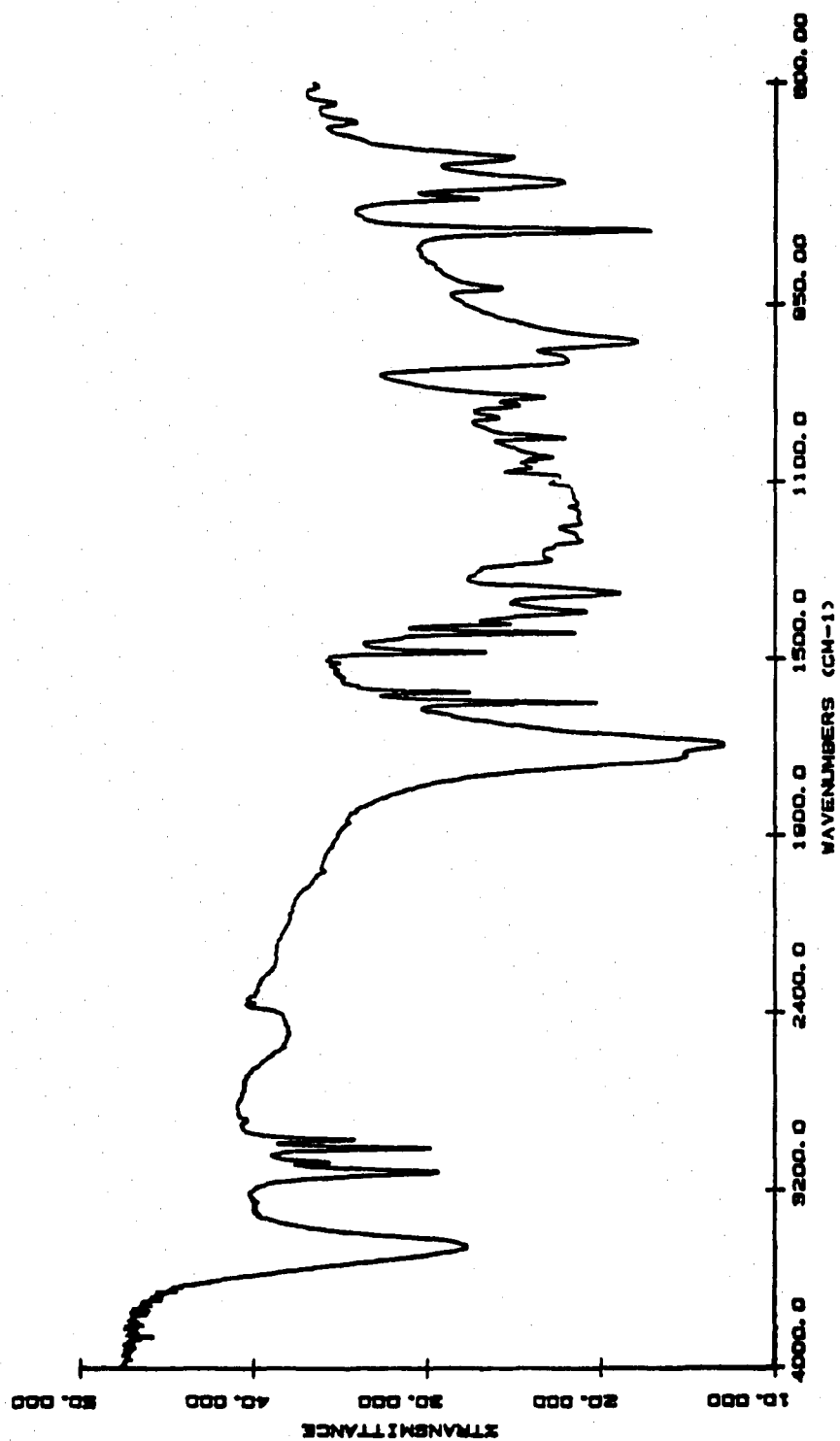


Figure 5. InfraRed Spectrum of PyIDA.

Table 9

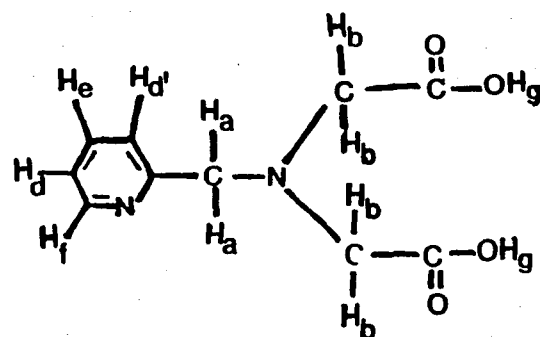
List of IR Frequencies for PyIDA Obtained From Nicolet 5DXB FT IR Spectrophotometer.¹

Wave numbers, cm ⁻¹	Functional Group
3425 (m)	(O-H) _{stretch} , Carboxylic hydrogen
3072, 3040 (m)	(C-H) _{stretch} , Aromatic
2976, 2944 (m)	(C-H) _{stretch} , Aliphatic
1720, 1691 (s)	(C=O) _{stretch} , Carboxylic
1594, 1572 (s)	(C=C) _{stretch} , Aromatic
148, 1439 (s)	(-CH ₂ -) _{bend}
1350 (s)	(C-N) _{bend} , Amine
997 (s)	(C-N) _{bend} , imide
832, 892 (s)	(C-H) _{bend} , aromatic

¹ m, s stand for medium and strong absorption, respectively.

Appendix B

H-NMR Spectrum of PyIDA



Chemical Shifts (ppm)

- | | |
|-------------------------------------|---------------------|
| a. 3.61 (singlet) | e. 8.02 (multiplet) |
| b. 4.28 (singlet) | f. 8.45 (multiplet) |
| c. 4.62 (singlet), H ₂ O | |
| d, d'. 7.51 (multiplet) | g. >10 |

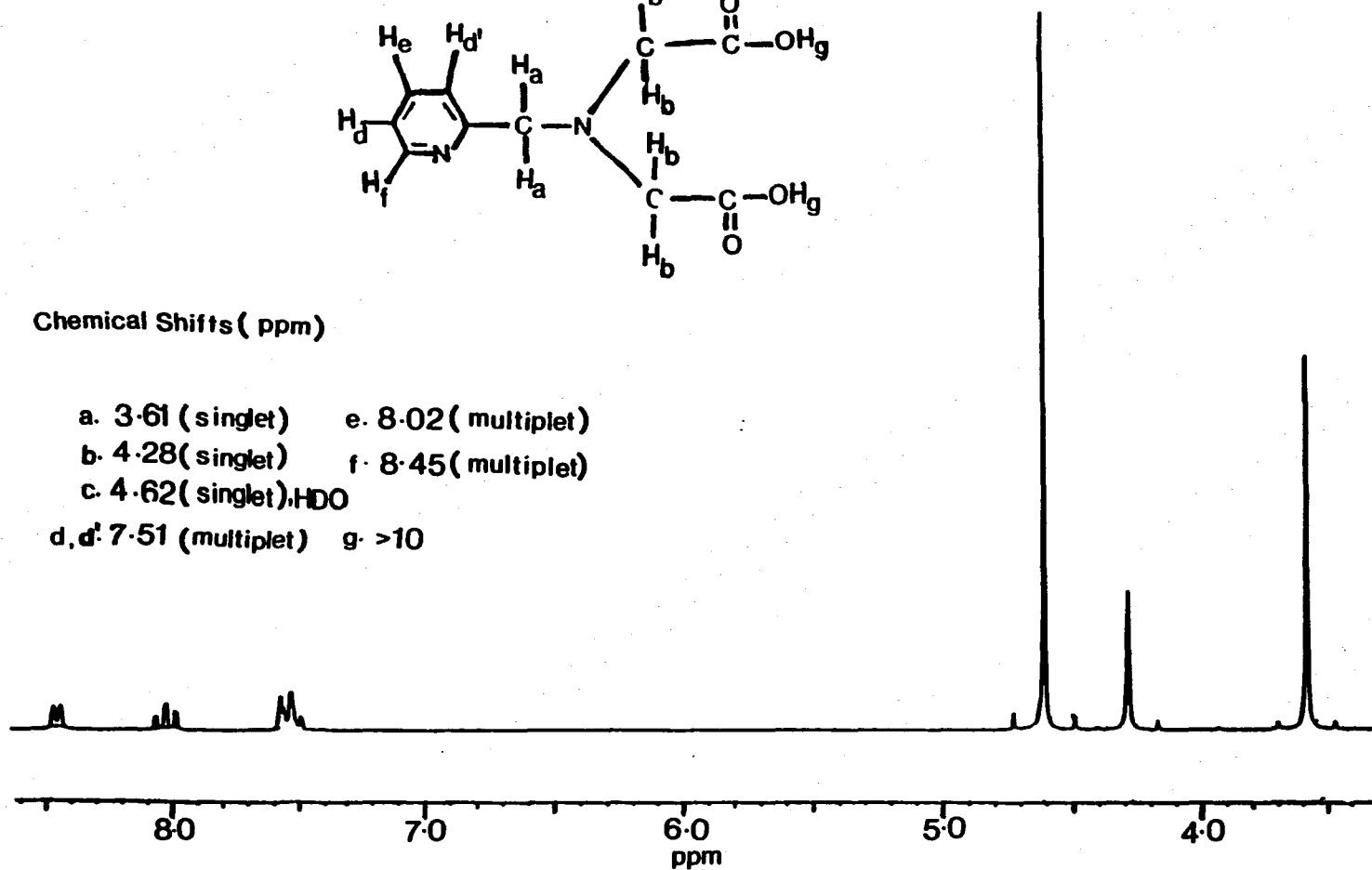


Figure 6. ^1H -NMR Spectrum of PyIDA Using FTNMR (200MHz, D_2O), and DSS (2,2-dimethyl-2-silapetane-5-sulfonic acid), as a reference.

Appendix C

Molar Absorptivity as a Function of Wavelength for CuPyIDA, Cu(II), NiPyIDA, Ni(II)

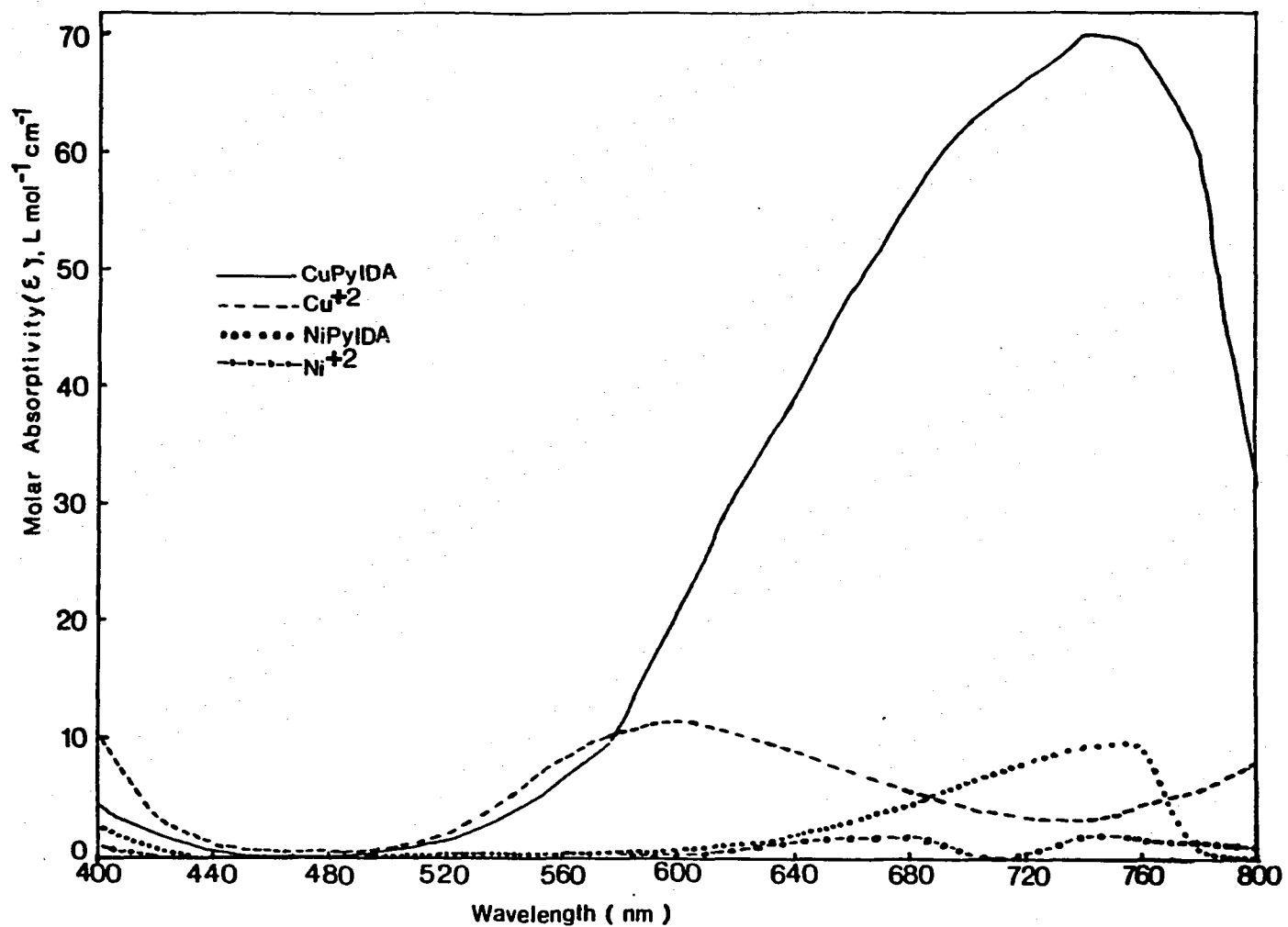


Figure 7. Molar Absorptivity as a Function of Wavelength for CuPyIDA, $\text{Cu}(\text{II})$, NiPyIDA and $\text{Ni}(\text{II})$.

Table 10

Comparison Between Observed and Expected Absorbance Values for the Exchange Reaction of NiPyIDA with Cu(II). ¹

Number of Half-lives	A _{observed}	A _{expected}
1	0.0565	0.0595
2	0.0848	0.0982
3	0.0989	0.104
4	0.106	0.111
5	0.110	0.115
6	0.111	0.117
7	0.112	0.118

¹ pH = 2.75, μ = 1.25, half-life for the exchange reaction is 4.92 minutes. The Chi-Square value calculated is equal to 3.29×10^{-3} and Chi-Square value from the table at degree of freedom 6 and 95% confidence level is 1.64, which shows that there is no significant difference between the observed and expected absorbance values.

Appendix D

Concentration and Absorbance Relationships

CONCENTRATION AND ABSORBANCE RELATIONSHIPS

The relationship shown in equation 5 between $[NiPyIDA]$, the absorbance at any time t , A_t , the final absorbance, A_∞ , and the molar absorptivities of reactants and products is derived under two assumptions. First, it is assumed no stable intermediate is present, which was shown by calculating expected absorbances at various times of an exchange reaction and comparing them with the actual values. The absorbance at anytime, t is equal to the absorbance of the reactants left and of the products-formed, the comparisons are shown in Table 10 in the Appendix 3. The second assumption is that the Beer-Lambert Law is obeyed. Thus, equation 5 can be derived as follows,

$$A_t = \epsilon_{NiPyIDA} b [NiPyIDA]_t + \epsilon_{Cu} b [Cu^{+2}]_t + \epsilon_{Ni} b [Ni^{+2}]_t + \epsilon_{CuPyIDA} b [CuPyIDA]_t \quad (24)$$

$$\text{and } [Cu^{+2}]_t = [Cu^{+2}]_\infty + [Ni^{+2}]_t \quad (25)$$

$$[Ni^{+2}]_t = [Ni^{+2}]_\infty - [NiPyIDA]_t \quad (26)$$

$$[CuPyIDA]_t = [CuPyIDA]_\infty - [NiPyIDA]_t \quad (27)$$

Substitution of the expression in equations 25, 26, and 27 into equation 24 and rearrangement yields equation 28.

$$A_t = [NiPyIDA] b (\epsilon_{NiPyIDA} + \epsilon_{Cu^{+2}} - \epsilon_{Ni^{+2}} - \epsilon_{CuPyIDA}) + \epsilon_{Cu} [Cu^{+2}]_\infty + \epsilon_{Ni} [Ni^{+2}]_\infty + \epsilon_{CuPyIDA} [PyIDA]_\infty \quad (28)$$

$$\text{Since } A_{\infty} = \epsilon_{\text{CuPyIDA}} b[\text{CuPyIDA}]_{\infty} + \epsilon_{\text{Cu}} b[\text{Cu}^{+2}]_{\infty} + \epsilon_{\text{Ni}} b[\text{Ni}^{+2}]_{\infty} \quad (29)$$

and substitution of equation 29 in to equation 28, rearrangement and solving for $[\text{NiPyIDA}]$ gives the desired equation 5.

$$[\text{NiPyIDA}] = \frac{A_t - A_{\infty}}{b(\epsilon_{\text{NiPyIDA}} + \epsilon_{\text{Cu}^{+2}} - \epsilon_{\text{CuPyIDA}} - \epsilon_{\text{Ni}^{+2}})} \quad (5)$$

REFERENCES

1. T. J. Bydalek and D. W. Margerum, J. Am. Chem. Soc., 1961, **83**, 4326.
2. D. W. Margerum and T. J. Bydalek, Inorg. Chem., 1962, **1**, 852-856.
3. T. J. Bydalek and D. W. Margerum, Inorg. Chem., 1963, **2**, 678.
4. D. W. Margerum and T. J. Bydalek, Inorg. Chem., 1963, **2**, 683-688.
5. T. J. Bydalek and M. L. Bloomster, Inorg. Chem., 1964, **3**, 667-671.
6. T. J. Bydalak and A. H. Constant, Inorg. Chem., 1965, **4**, 833-836.
7. D. W. Margerum, D. L. Janes and H. M. Rosen, J. Am. Chem. Soc., 1965, **87**, 4463-4472.
8. R. K. Steinhaus and R. L. Swann, Inorg. Chem., 1973, **12**, 1855-1860.
9. D. L. Margerum, B. A. Zabin and D. L. Janes, Inorg. Chem., 1966, **5**, 250.
10. E. Mentasi and E. Pelizzetti, Inorg. Chem., 1978, **17**, 3133-3137.
11. R. K. Steinhaus and C. L. Barsuhn, Inorg. Chem., 1974, **13**, 2922-2929.
12. R. K. Steinhaus and S. H. Erickson, Inorg. Chem., 1980, **19**, 1913-1920.
13. R. K. Steinhaus, Inorg. Chem., 1982, **21**, 4084-4088.
14. R. K. Steinhaus and Z. Amjad, Inorg. Chem., 1973, **12**, 151.
15. R. G. La Coste and A. E. Martell, Inorg. Chem., 1964, **3**, 881.
16. H. Irving and J. J. R. F. Da Silva, J. Chem. Soc., 1963, 945-952.
17. L. C. Thompson, Inorg. Chem., 1964, **3**, 1015-1018.
18. J. C. Cassett and R. G. Wilkins, J. Am. Chem. Soc., 1968, **90**, 6045.
19. C. D. Hubbard, Inorg. Chem., 1971, **10**, 2341-2343.
20. D. W. Gruenwedel, Inorg. Chem., 1968, **7**, 495-501.
21. N. Tanaka, H. Osawa and M. Kamada, Bull. Chem. Soc. Jpn., 1963, **36**, 530.
22. D. W. Margerum, P. J. Meriardi and D. L. Janes, Inorg. Chem., 1967, **6**, 283.

23. G. F. Smith and D. W. Margerum, Inorg. Chem., 1969, 8, 135-138.
24. R. J. Magee, W. Mazurek, M. J. O'Connor and A. T. Philip, Aust. J. Chem., 1964, 27, 1885.
25. G. Kohler and H. Elias, Inorg. Chim. Acta., 1979, 34, L215-L218.
26. R. L. Shriner, R. C. Fuson and D.Y. Curtin, The systematic Identification of Organic Compounds. A Laboratory Manual, 4th ed., John Wiley & Sons Inc., New York, 1959. p426
27. J. P. Jones, E. J. Billo, and D. W. Margerum, J. Am. Chem. Soc., 1970, 92, 1875.
28. M. Eigen, Pure Appl. Chem., 1967, 6, 97.
29. L. G. Sille'n and A. E. Martell, Stability Constants of Metal Ion Complexes, Supplement No. 1, Special publication No. 25. The Chemical society, London, 1971. p865
30. L. G. Sille'n and A. E. Martell, Stability Constants of Metal Ion Complexes, Special publication No. 17, The Chemical Society, London, 1964. p754
31. A. E. Martell and R. M. Smith, Critical Stability Constants. Vol. 1 Amino Acids. Plenum Press, New York, 1974. p469
32. D. W. Margerum, D. B. Rorabacher and J. F. G. Clarke, Jr., Inorg. Chem., 1963, 2, 667-677.
33. D. W. Margerum, C. W. Cagley, D. C. Weatherburn, G. K. Pagen kopt, Coordination Chemistry, A. E. Martell, ed. American Chemical Society, Washington, D.C., 1978, ACS monograph, 174. p10-11.
34. D. W. Margerum and M. Eigen, Proceedings of the 8th International conference on coordination chemistry, Springer-Verlag, Vienna, 1964. p289